Expression levels of α5 subunit-containing GABA-A receptors in the prelimbic cortex are associated with visual perceptual learning

Matthew C. D. Bailey[1], Emilie Preisler[1], Clara Valazquez Sanchez[1], Lucia Marti Prats[1], Olivia Stupart[1], Livia J.F. Wilod Versprille[1], Johann F. du Hoffmann[2], Zoe Kourtzi[1], Jeffrey W. Dalley[1,3,#]

1 Department of Psychology, University of Cambridge, Downing St, Cambridge CB2 3EB, UK; 2 Boehringer Ingelheim Pharma GmbH & Co. KG, Div. Research Germany, Biberach an der Riβ, Germany; 3 Department of Psychiatry, Herschel Smith Building for Brain and Mind Sciences, University of Cambridge CB2 0SZ, UK

Short title: Inhibitory modulation of visual perceptual learning

Word count: 5,707
Abstract: 219
Introduction: 583
Discussion: 1,853
Figures: 5

Author for correspondence: Professor Jeffrey W. Dalley, Department of Psychology, University of Cambridge, Downing St, Cambridge CB2 3EB, UK. Tel. +44(0)1223 765 291; Email: jwd20@cam.ac.uk

Abstract

Perceptual learning is a temporally dynamic process involving the acquisition and integration of sensory information necessary for adaptive decision making. Resolving the neural basis of perceptual learning could uncover new therapeutic targets for schizophrenia and other neurodevelopmental disorders that implicate impaired perceptual acuity. In the present study, we developed a novel touchscreen task which utilizes orientation discrimination to assess visual perceptual learning (VPL) in male and female rats. Based on previous evidence we hypothesised that VPL would depend on inhibitory neurotransmission mediated by γ-amino butyric acid (GABA). Segregating subjects based on 'poor learning' (lower tertile) and 'good learning' (upper tertile) revealed dose-dependent improvements in VPL in poor learners following the administration of a GABA-B agonist (R-baclofen) and an α5 subunit specific GABA-A (GABRA5) positive allosteric modulator (alogabat) administered early in learning. Poor VPL performance was associated with a significant reduction in GABRA5 expression in dorsal regions of the prefrontal cortex (PFC), most notably the prelimbic cortex. Reduced GABRA5 expression in this region was co-localized to somatostatin- and parvalbumin-expressing interneurons. These findings indicate that inter-individual variation in the expression of GABRA5 in selective PFC populations of inhibitory interneurons may determine the speed and acuity of VPL. Based on these findings, interventions that restore GABRA5 signalling in the PFC may hold therapeutic relevance for neuropsychiatric disorders involving deficits in perceptual learning.

Key words: GABA; adaptive decision making; spatial transcriptomics; primary visual cortex; prefrontal cortex; parvalbumin interneurons

1.0 Introduction

Visual perceptual learning (VPL) refers to long-term improvements in visual discrimination that emerge after repeated training. Previous studies have revealed finely tuned stimulus- and context-specific cortical responses during VPL[1–4]. Such responses are linked to synaptic plasticity in primary visual cortex (V1) with intrinsic neurons exhibiting small receptive fields and narrow feature selectivity[5–7]. Higher visual processing areas including parietal and frontal cortices involved in decision-making and attention are progressively also recruited alongside classical visual processing areas such as V1 and superior colliculus to refine behavioral output and improve visual discrimination[8–10]. However, the relative contributions of bottom-up sensory *versus* top-down decisional and attentional control in VPL remain poorly understood.

Inhibitory control is fundamental to reshaping cortical circuits throughout development and adulthood, coordinating plasticity during sensitive periods[11,12] and VPL[13–16]. γ-Aminobutyric acid (GABA), the primary inhibitory neurotransmitter in the brain acts in concert with glutamate, the primary excitatory neurotransmitter, to regulate local circuit and global network excitability *via* the excitatory-inhibitory balance (E/I). Dysregulated E/I balance is associated with perceptual deficits in neurodevelopmental disorders such as autism [17,18] and schizophrenia[19–21], with aberrant inhibition driving network abnormalities[22–27]. Resolving the mechanism by which inhibition contributes to VPL may thus inform the development of new interventions to improve perceptual learning in a variety of disorders.

At the cortical circuit level, distinct populations of inhibitory interneurons contribute to experience-dependent remodelling of sensory, associative and executive networks recruited during learning and attentional tasks[28–31]. These include parvalbumin (Pvalb)-, somatostatin (Sst)-, and vasoactive intestinal peptide (VIP)- expressing neurons in V1, which dynamically remap their activity as VPL proceeds[31–35]. During late stages of learning, increased attentional engagement recruits higher-order inhibitory microcircuits to sharpen stimulus selectivity and enhance network fidelity[36–39]. However, within these microcircuits, GABAergic interneurons exhibit significant receptor and receptor composition heterogeneity and are recruited in a context dependent manner to modify network excitability[40–43].

Given the established role of the α5 subunit containing GABA-A receptor (GABRA5) in hippocampal-dependent learning and memory[44–47], the present study investigated the potential of GABRA5 to enhance VPL. Although GABRA5 represent less than 5% of

cortically expressed GABA-A receptors, they are expressed both intra- and extra-synaptically and thus contribute respectively to phasic and tonic inhibition[45,48,49]. GABRA5 receptors also show dynamic activity-dependent synaptic re-localisation, a process hypothesised to facilitate fine tuning of tonic and phasic inhibitory tone to preserve learned associations in a context dependent manner[50]. Thus, modulation of GABRA5 receptors may offer a promising strategy to rescue or enhance visual perceptual learning in autism, schizophrenia and other neurodevelopmental disorders.

To investigate the role of GABRA5 in VPL we established a novel touchscreen task for rats involving the discrimination of visual gratings with distinct orientations. We compared sex-differences in task acquisition and baseline performance before testing the sensitivity of the task to a range of GABAergic compounds that affect distinct aspects of GABAergic synaptic transmission and stratified these effects according to poor and good learning performance on the task. Given that the rate of learning in visual touchscreen discrimination tasks is linked to thresholds of visual acuity[51] we also investigated the dimensional relationship of VPL in individual animals and expression levels of the GABRA5 mRNA transcript and protein product in V1 and frontal cortex. We hypothesised that enhancing GABAergic inhibition with selective GABA reuptake inhibition (tiagabine) and a positive allosteric modulator of GABRA5 (alogabat)[52] would enhance VPL. We further hypothesised that inter-individual variation in VPL would relate to GABRA5 expression with faster visual perceptual learning in animals exhibiting increased GABRA5 expression.

2.0 Methods

2.1 Subjects

Thirty-two Lister-hooded rats (16 male, 16 female) were raised from time mated dams (Envigo, Bicester, UK), weaned at post-natal-day (PND) 21, and housed in groups of four with environmental enrichment under a 12/12hr reverse light/dark cycle (lights on 6am). From weaning, animals had *ad libitum* access to food (Safe A40, Germany) and water. After PND26, animals were handled 3 times per week to habituate them to human contact. On PND56 animals were food restricted to no less than 85% free feeding weight for the remainder of the experiment. Animals were weighed at least once per week. Animals were sacrificed at the end of the experiment by schedule 1 methods for tissue collection. All procedures were carried out in accordance with the UK (1986) Animal (Scientific

Procedures) Act (PPL PP9536688) and were approved by the University of Cambridge Animal Welfare and Ethical Review Body (AWERB).

2.2 Visual perceptual learning task

Operant chambers running K-Limbic software (Med Associates, UK) were integrated with a 1024x768 resolution portrait touchscreen (Nexio, UK) on one wall, and a food magazine with light, pellet dispenser, house light, and tone generator on the opposite wall (see Figure 1A). A camera was installed overhead to record behavior.

To investigate VPL, a novel 3-stimuli orientation-based visual discrimination paradigm adapted from Horner and colleagues[53] was developed using sinusoidal stimuli presented in three equally spaced response windows (200x200 pixels), located 150 pixels from the bottom of the touchscreen. Target stimuli were assigned at the beginning of training, counterbalanced within the cohort (16 animals 0°, 16 animals 90°) and spatially randomised on a trial-by-trial basis to reduce procedural learning and location bias. Pretraining proceeded with chamber acclimatisation with reward pellets (TestDiet AIN-76, 5TUL, Cat No.1811155) (PT1), appetitive autoshaping to the touchscreen by association of target grating with reward (PT2), timeout for background touches (PT3), and the introduction of distractors in the form of two blank stimuli (PT4). Criteria for progression was >80% correct on 2 sessions (see Figure S1).

Animals then completed a series of visual discrimination training sessions to assess the suitability of chosen angular separations from target (ang_sep) before moving to the final task. Beginning with a 90° (VD1) separation from the target stimuli, training progressed by decreasing the separation angle through 45°, 30°, 15° and finally 10° (VD5). Animals were advanced to the next training stage depending on difficulty after 2 consecutive sessions at criteria: >80% 90°→45°, >70% 45°→30°, >60% 30°→15°, >50% 15°→10°, >50% 10°→final task. Animals that reached VD5 but failed to reach criteria after 5 sessions were deemed to have reached their perceptual limit. All animals were moved to the final task for pharmacological interventions.

The final task involved 150 trials split into five, 30-trial blocks of distractor orientation which converged on the target stimulus orientation (Easy - 90°, 45°, 30°, 15° and 10° - Hard – in degrees from target angle). On any given trial, three stimuli were presented, one target grating, one distractor grating, and one white stimulus randomised on a trial-by-trial basis. Here, target distractor distance (TDD) was classified as ‘close’ when target grating and

distractor grating were presented in adjacent windows, and 'far' when target distractor gratings were separated by the third, white stimuli. TDD was employed to investigate the role of attentional load and simultaneous suppression of multiple stimuli on perceptual decision making. A correct response was rewarded with a sucrose pellet and auditory tone whereas incorrect responses at either the distractor stimuli (distractor grating or white) or background were signalled with a 10s house light pulse timeout and no food reward. Sessions lasted on average 1 hour with an inter-trial-interval (ITI) of 10s (see Figure 1B, C). For further details of the training stages and task contingencies refer to Figure S1.

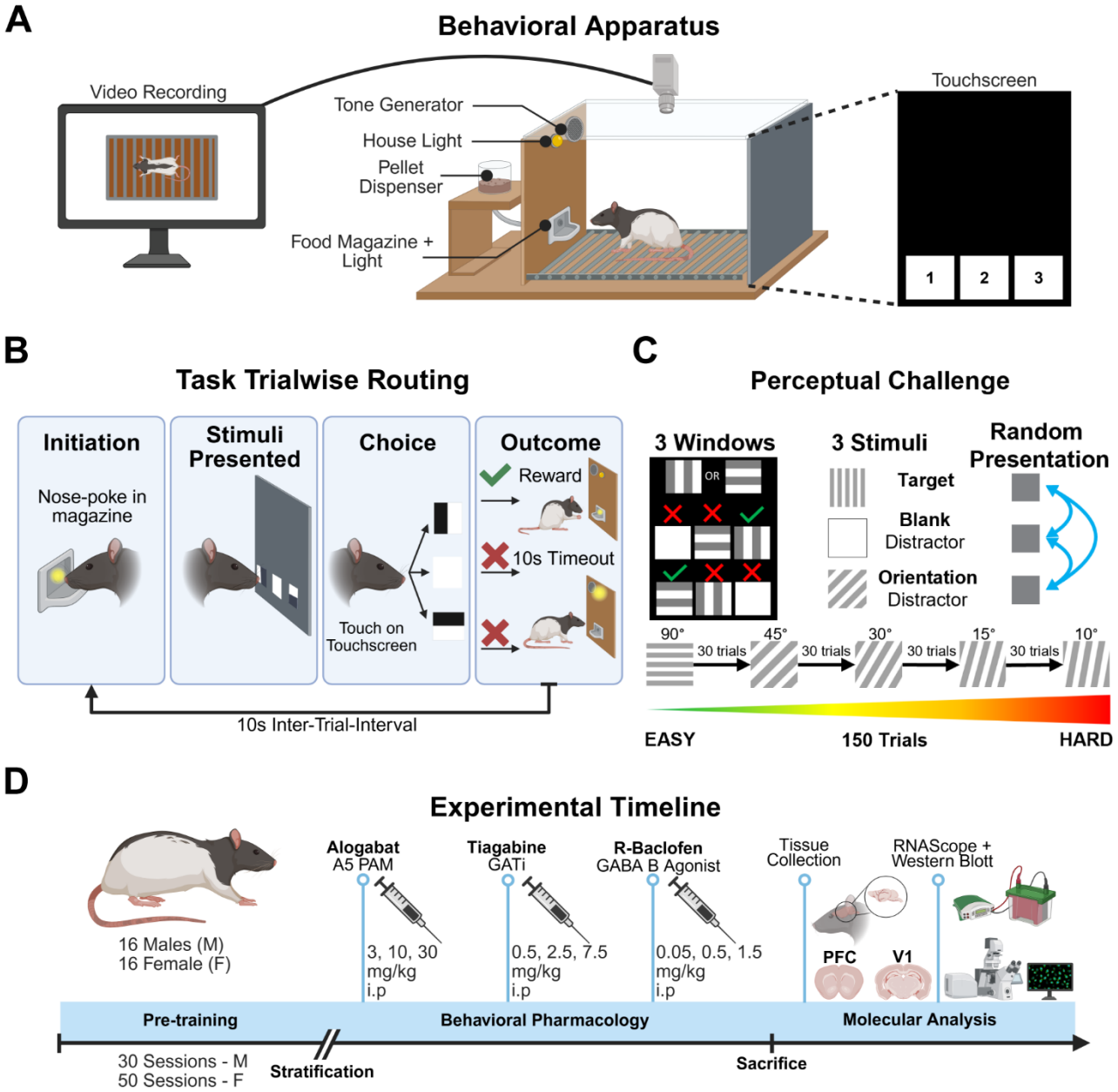

Figure 1 : Visual discrimination task and experimental timeline
A Operant chamber apparatus. Med Associates chambers showing the position of the house-light, tone generator and food magazine with a light connected to a pellet dispenser on one side of the chamber and a 1024 x 768 resolution touchscreen on the other. A CCTV camera was mounted overhead to record behavior. **B** Trial wise decomposition of final task contingencies. A nose poke in the illuminated food magazine initiated a trial. Stimuli were then presented on the touchscreen (1 target grating, 2 distractors (1 blank, 1 grating) with animals making a choice between the 3 presented stimuli. A correct response was reinforced with a sugar pellet paired with tone (magazine light on during collection). Incorrect responses at either the distractor or background stimuli received a 10 second timeout with no reward and house light illumination. **C** Baseline task perceptual challenge and distractor presentation sequence. In total, the task consisted of 150 trials in blocks of 30 at each distractor frequency, starting at 90° from target. Stimuli were presented randomly on a trial-by-trial basis. **D** Experimental timeline showing behavioral stratification, pharmacological challenges and molecular analyses. Figure created using https://app.biorender.com/

2.3 Subject stratification

To investigate individual differences in visual perceptual learning, animals were stratified into ‘learning type’ groups based on their task acquisition rate. For males (n=16), animals that completed pretraining and VD training during the thirty-three-session training period were classified as “good learners” (n=5), whereas animals that failed to reach visual discrimination training were classified as “poor learners” (n=6). Animals that completed pretraining but did not finish VD training were classed as “intermediate learners” (n=5) and represented the mean task acquisition rate. Only good and poor learners were considered for final analysis to investigate what drives good vs poor VPL.

Although females were included in the study, it was not possible to use the same stratification procedure as males because considerably more sessions were required for females to acquire the task (mean 52 sessions) and baseline task response rates were variable. Moreover, females trained on the basic discrimination task failed to complete the more difficult training stages of the VPL task, as shown in Figure S2, meaning that no animals were classed as ‘good learners’ despite the extended training period. Instead, most females were classed as ‘poor’ (n=8), with the remainder which either reached criterion on the PT4, or begun VD training were classed as ‘intermediate’ (n=8). These groups were used in comparing within-sex performance, pharmacology and molecular variations, and can be found in the supplementary material section.

2.4 Pharmacological interventions

Selective GABAergic compounds were administered according to a Latin square design. The compounds (and doses) were tested in with a 3-day dosing schedule (day 1 (dose level 1), day 2 (no drug), day 3 (baseline) and at least 3 day washout period between each compound: (1) alogabat (3, 10, 30 mg/kg) (2) tiagabine hydrochloride (0.5, 2.5, 7.5 mg/kg); (3) R-baclofen (0.05, 0.5, 1.5 mg/kg). Alogabat (provided by Boehringer Ingelheim Pharma, Germany) was administered in 5% HCl (1M) and 95% 2-(hydroxypropyl)-β-cyclodextrin (20%) at 2 ml/kg (pH 7-7.5). Tiagabine-HCl (Insight Biotechnology, UK-CAS 145821-59-6) was administered in deionised water pH 7-7.5 at 1 ml/kg. R-Baclofen (Insight Biotechnology, UK-CAS 69308-37-8) was administered in 0.9% saline (pH 7-7.5) at 1 ml/kg. Tiagabine and R-baclofen were administered simultaneously to male and female animals, whilst alogabat was administered first to males, and as the final compound to females, accounting for the time difference in pertaining. All drugs were administered *via* intraperitoneal (i.p.) injection with 30-minute pretreatment time (See Figure 1D and Figure S10 for further details).

2.5 Tissue collection

Rats were anesthetised with isoflurane (Sigma-Aldrich, UK) *via* inhalation before decapitation 5 days after the final VPL session. Brains were collected and snap-frozen with dry-ice pre-cooled isopentane (Sigma-Aldrich, UK) and stored at -80°C. Brains were sectioned using a cryostat (Leica, UK) to obtain coronal slices of the medial prefrontal cortex (mPFC) (5.16 to 2.28 mm from Bregma) and V1 (-5.6 to -9.1 mm from Bregma). Each hemisphere was prepared for Western blotting (WB) with sections cut at 200 µm or RNAscope *in situ* hybridisation (RNAScope) with sections cut at 12 µm. Hemispheres were counterbalanced between the two assays, and slices were mounted on Menzel gläzer superfrost® slides (Thermo Fisher Scientific, UK) for WB or Superfrost® plus slides (Thermo Fisher Scientific, UK) for RNAscope. Sections were stored at -80°C prior to processing.

2.6 Western immunoblot analysis

WB were conducted using a WB kit according to manufacturer guidelines (Invitrogen-Life Technologies, UK). Four regions-of-interest (ROI)s were extracted from the slices of each rat: V1, Cg1, PrL, and IL. After immunoblotting, GABRA5 expression was developed using a primary antibody for GABRA5 (Biorbyt, UK – 1:1000 Cat No. orb374299) incubated

overnight at 4°C on a shaker. The primary antibody for the housekeeping protein actin (Abcam, UK – 1:10,000 Cat No. ab8226) was incubated for 1h at room temperature. Secondary antibodies, IRDye680RD and IRDye800CW (LI-COR, UK – 1:15,000 Cat No: 680, 926-68071; 800, 926-32210) were incubated at room temperature for 1h alongside a chameleon duo ladder (LI-COR, UK – Cat No. 928-60000) before imaging (Odyssey Imaging System, LI-COR, UK).

2.7 RNAscope fluorescence in-situ hybridisation

The spatial transcriptomic profile of GABRA5 in the mPFC and V1 was assayed in replicate samples to investigate cell-type specific GABRA5 mRNA expression. The assay and target probes were performed[54] according to the fresh frozen tissue protocol provided by the manufacturer (RNAscope fluorescent multiplex reagent kit, ACD, UK) with specific details given in the supplementary section (Table 1).

Tissue was imaged using a Zeiss Axio Imager M2 microscope with an AxioCam MRm microscope camera (Oberkochen, Germany) running Visiopharm software (Medicon Valley, Denmark). Approximately 15 images were each taken of V1 and mPFC subregions (cingulate cortex - Cg1; prelimbic cortex – PrL; infralimbic cortex - IL) with 20X magnification. Signals were quantified using an RNAscope signal analysis pipeline developed by Velazquez-Sanchez et al.[55], which utilised a MATLAB script (The MathWorks Inc) combined with a FIJI/ImageJ[56] machine learning algorithm to count mRNA molecules within DAPI labelled cells.

2.8 Data analysis

Behavioral data were collected on a trial-by-trial basis and pre-processed to remove outliers. Baseline outliers were removed based on the following criteria: <96/150 trials completed in each session – only reaching the third block of distractor, and response latencies (<100ms) that were too fast to be instrumental in nature (e.g. arising from unintentional tail contacts with the touchscreen). For the pharmacological experiments, outliers were removed for failed/incomplete dosing or a failure to reach the trial completion criteria on <2/4 doses of each compound (n=1 removed per compound), final n: n=5 poor learners, n=5 good learners. Reaction time responses were inverse transformed (-100/RT) to normalise distribution of the data and facilitate more robust modelling.

Statistical comparisons were made in R (Version 4.4.2)[57] using within-subjects mixed-effects modelling, a generalised logit link function to quantify trial wise accuracy, and a

linear model to analyse inverse transformed mean response latencies (inverseRT). Fixed-effects relationships between angular separation from target (ang_sep), sex, learning type (LT) and target distractor distance (TDD) were investigated. Animal ID was added as a random effect with a random intercept to account for within group individual variation (see Figure S3). Pharmacological models were similar, although model selection showed TDD did not have significant explanatory power and was therefore not included in the final model. Ang_sep was also only included as a fixed effect rather than interaction due to model convergence violations. Where appropriate, estimated-marginal-means pairwise comparisons with Tukey HSD correction were performed and reported as log-odds ratios for generalised models.

The analysis of Western blot data was carried out using Welch's two sample t-test to compare learning type means within cortical region. A within-subjects linear mixed-effects model was applied to molecular data to investigate the relationships between learning-type and GABRA5 mRNA expression within specified cell types in the various brain regions of interest. Each animal was added as a random effect with a random intercept to account for within group individual variation. An ANOVA was performed to identify main effects, and where appropriate, estimated-marginal-means pairwise comparisons with Tukey HSD correction were performed between groups within region, within cell type, and adjusted p values ≤ 0.05 reported (see Figure S4). All variables and models were performed and evaluated for analysis suitability using normality and model evaluation metrics available in the Performance package in R (see Figure S5). Full summaries of statistical models can be found in supplementary table 2.

3.0 Results

3.1 Modelling VPL with a novel orientation discrimination task

Assessment of performance on the baseline version of the VPL task revealed that narrowing the angular separation from the target stimulus decreased discriminative accuracy (Figure 2A) (Compared to ang_sep90: ang_sep45: $Pr(>|z|) = 0.970$, ang_sep30: $Pr(>|z|) = 2.14e^{-05}$, ang_sep15: $Pr(>|z|) < 2e^{-16}$, ang_sep10, $Pr(>|z|) < 2e^{-16}$). Here there was also a within-block sex difference in trial wise mean accuracy where females displayed lower accuracy from block 2 onwards (ang_sep90, F-M: adj.p value = 0.418, ang_sep45, F-M: adj.p value = 0.0471 ang_sep30, F-M: adj.p value = 0.0531 ang_sep15, F-M: adj.p value = 0.0275, ang_sep10, F-M: adj.p value = 0.0247). However, the accuracy of males and females across all blocks was not significantly different (Compared to F: M: $Pr(>|z|) = 0.732$) (Figure 2B). When the relative location of the target and distractor gratings was considered (Target Distractor Distance – TDD), both sexes were impaired by a greater distance between stimuli (F, TDDclose – TDDfar: adj.p value = <.0001. M, TDDclose – TDDfar: adj.p value = 0.0002), with females showing a greater reduction in accuracy than males (TDDfar, F-M: adj.p value = 0.02) (Figure 2C). There was no such effect with close TDD (TDDclose, F-M: adj.p value = 0.163). Analysis of concordant inverse transformed response latencies (inverseRT) revealed a slowing of responses with narrowing angular separation (Figure 2D) ($F(_{4,269}) = 123$, $Pr(>|z|) < 2.2e^{-16}$) and a modest blockwise sex effect (ang_sep90, F-M: adj.p value = 0.848, ang_sep45, F-M: adj.p value = 0.363, ang_sep30, F-M: adj.p value = 0.204, ang_sep15, F-M: adj.p value = 0.0696, ang_sep10, F-M: adj.p value = 0.0781 (Figure 2E). However, there was no significant difference between males and females on inverseRT across the full task ($F(_{1, 29}) = 1.54$, Pr(>F) 0.225) or when analysed by TDD (Sex:TDD interaction, $F(_{1, 269}) = 0.224$, Pr(>F) = 0.637 (Figure 2F).

Figure 2: Baseline performance measures on the VPL task
A Trial-wise mean accuracy by sex presented as mean ± SEM. Dashed lines denote distractor frequency blocks. Annotations denote between-sex comparisons within each distractor frequency block. **B** Distribution of baseline task accuracy segregated by sex. Each data point denotes an individual animal. **C** Distribution of mean task accuracy for each target distractor distance (TDD). Comparisons made within TDD-between sex and within sex-between TDD. **D** Trial-wise mean inverseRT by sex presented as mean ± SEM. Dashed lines mark distractor frequency blocks. Annotations denote between-sex comparisons, within distractor frequency block. **E** Distribution of mean inverseRT segregated by sex. Each data point denotes an individual animal **F** Distribution of mean inverseRT by TDD. Comparisons made within TDD-between sex and within sex-between TDD.
Baseline sessions displayed for each sex with statistical comparisons made by generalized linear mixed-effects model with binomial link for accuracy (**A-C).** Linear mixed-effects model for inverseRT (**D-F)**. Boxplots denote median, interquartile range with whiskers extending to 1.5x IQR. Outliers denoted by solid points. Pairwise comparisons made via estimated-marginal-means to “Female” condition in each case, within block **(A,D)** and “close” **(C,F)**. Effect sizes: “p value” = p<0.1, “*” = p<0.05, “***” = p<0.001 **(D-F)** as log-odds ratios **(A-C)**.

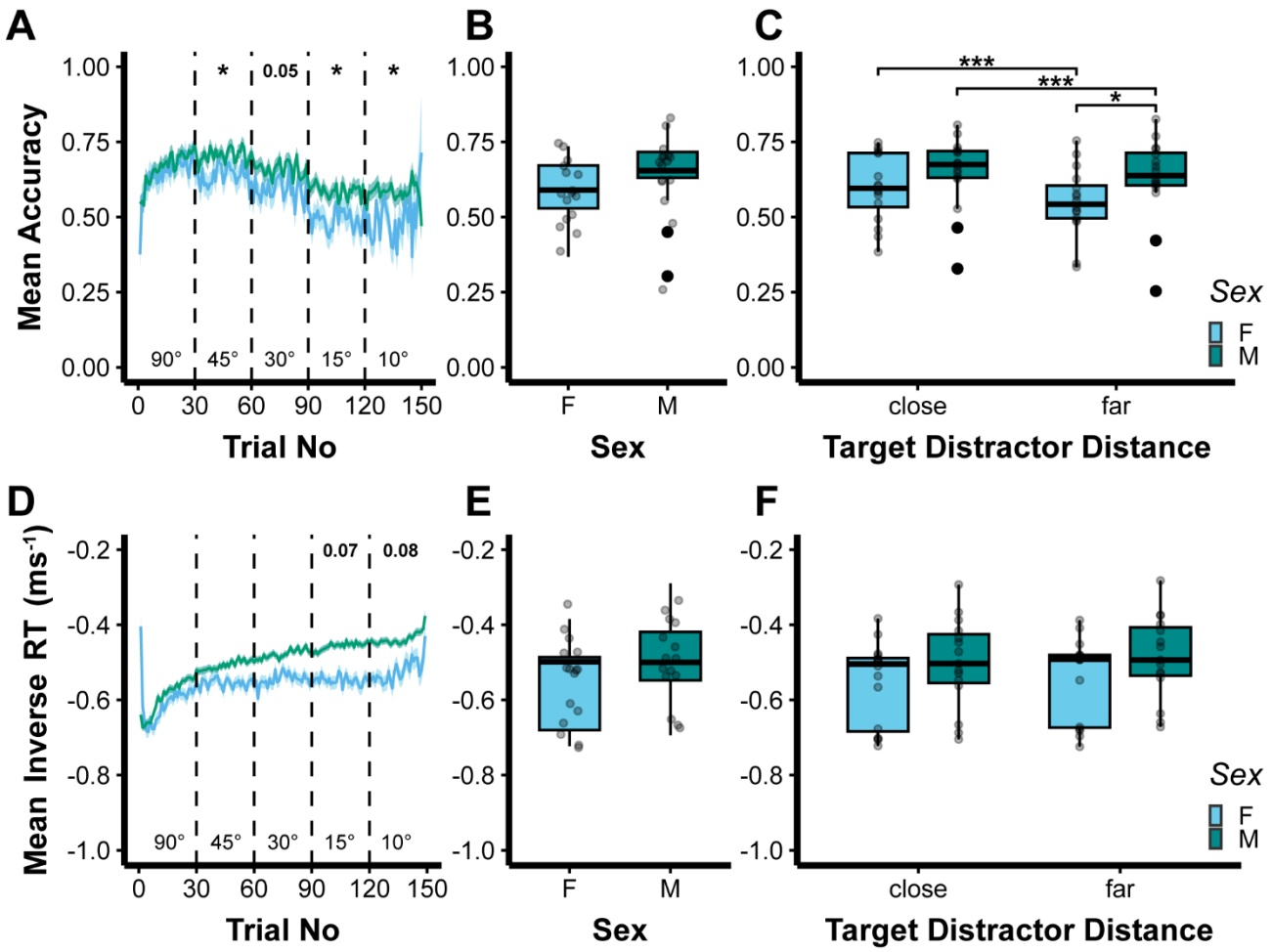

3.2 Segregation of good *versus* poor learners on the VPL task

After validating the perceptual challenge of our paradigm, subjects were stratified based on their VPL performance. Given that, for difficult learning paradigms, rodents require extensive training and are often over trained by the time they are evaluated at baseline, we segregated animals during the task acquisition stage. To achieve this, we grouped subjects by their final training stage before the drug challenges. Those which completed all pretraining, reaching the baseline task were classed as “Good Learners” (n = 5), those which did not complete pretraining were “Poor Learners” (n = 6) (Figure 3A). Unfortunately, due to differing pre-training exposures, we could not directly compare sexes with this stratification approach, instead we completed a concordant stratification analysis for female animals available in the supplementary materials (Figures S7, S8, S9).

In males, groupwise comparisons revealed within-block learning differences in accuracy (Figure 3B) where good learners were more accurate than poor learners in all but the final block (ang_sep90, poor-good: adj.p value = 0.0166, ang_sep45, poor-good: adj.p value =

0.0057, ang_sep30, poor-good: adj.p value = 0.0083, ang_sep15, poor-good: adj.p value = 0.0095, ang_sep10, poor-good: adj.p value = 0.169).This was associated with good learners displaying a greater full task accuracy (Figure 3C) (poor – good: Pr(>|z|) = 0.0253) and both TDD close and far accuracies than poor learners (Figure 3D) (TDDclose, Poor-Good: adj.p value = 0.0258, TDDfar, Poor-Good adj.p value = 0.0114). Additionally, whilst poor learner accuracy was negatively impacted by increased TDD, good learners displayed only a marginal reduction in performance between TDDclose and TDDfar trials (Poor, TDDclose – TDDfar: adj.p value <.0001, Good, TDDclose – TDDfar: adj.p value = 0.0599).

Analysis of inverseRT highlighted no blockwise (Figure 3E) (ang_sep90, Poor-Good: adj.p value = 0.263, ang_sep45, Poor-Good: adj.p value = 0.203 ang_sep30, Poor-Good: adj.p value = 0.17, ang_sep15, Poor-Good: adj.p value = 0.204, ang_sep10, Poor-Good: adj.p value = 0.254) or taskwise (Figure 3F) differences between learning types (poor – good: $F_{(1, 9)}$ = 1.81, Pr(>F) = 0.212. There were also no within or between group effects of TDD on inverse RT (Figure 3G) ($F_{(1, 89)}$ = 0.558, Pr(>F) = 0.457).

Figure 3: Summary measures of perceptual performance on the VPL task
A Summary of stratification procedure based on training stage reached at the end of 33 sessions of pretraining (males only). **B** Trial-wise mean accuracy by learning type presented as mean ± SEM. Dashed lines mark distractor frequency blocks. Annotations denote between-learning type comparisons, within distractor frequency block. **C** Distribution of baseline accuracy by learning type. **D** Distribution of mean accuracy segregated by target distractor distance. Points denote individual animals per TDD. Comparisons made within TDD-between learning type and within learning type-between TDD. **E** Trial-wise mean inverseRT by learning type presented as mean ± SEM. Dashed lines mark distractor frequency blocks. Annotations denote between-learning type comparisons, within distractor frequency block. **F** Distribution of mean inverseRT by learning type.
G Distribution of mean inverseRT by target distractor distance. Points denote individual animals per TDD. Comparisons made within TDD-between learning type and within learning type-between TDD. Baseline sessions are displayed for each learning type with statistical comparisons made by generalized linear mixed-effects model with binomial link for accuracy (**B-D).** Linear mixed-effects model for inverseRT (**E-G)**. Boxplots denote median, interquartile range with whiskers extending to 1.5x IQR. Outliers denoted by solid points. Pairwise comparisons made via estimated-marginal-means to “Poor learner” condition in each case, within block **(B,E)** and “close” **(D,G)**. Effect sizes: “*” = p<0.05, “**” = p<0.01**(E-G)** as log-odds ratios **(B-D)**.

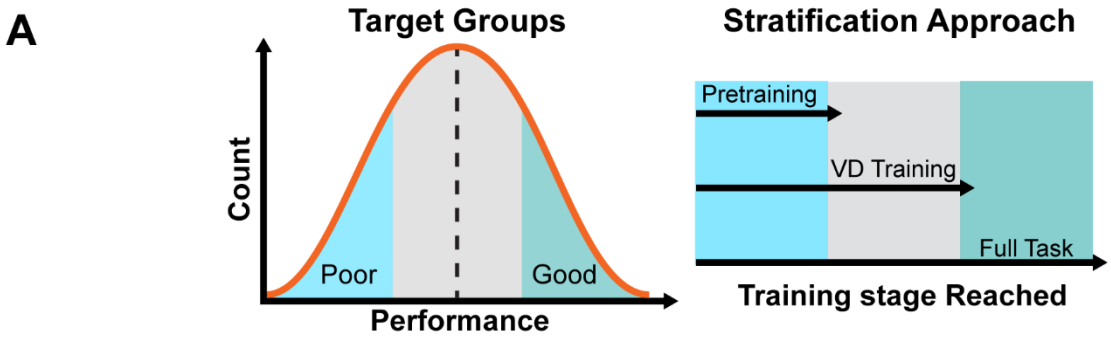

Learning Type	Criteria	Total Animals
Poor Learner	Failed complete Pre-training	6
Good Learner	Reached final task	5

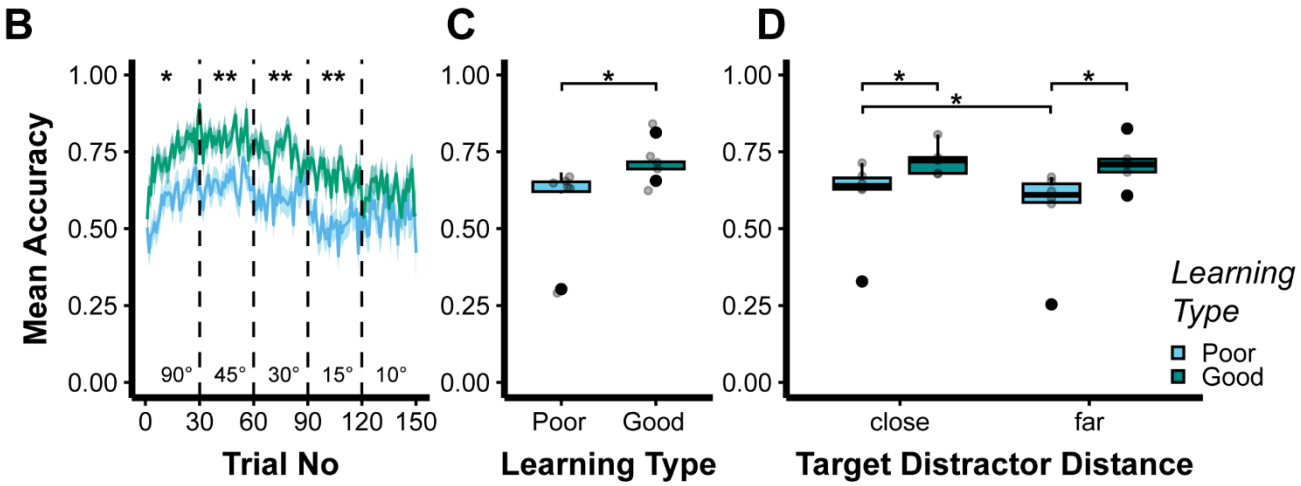

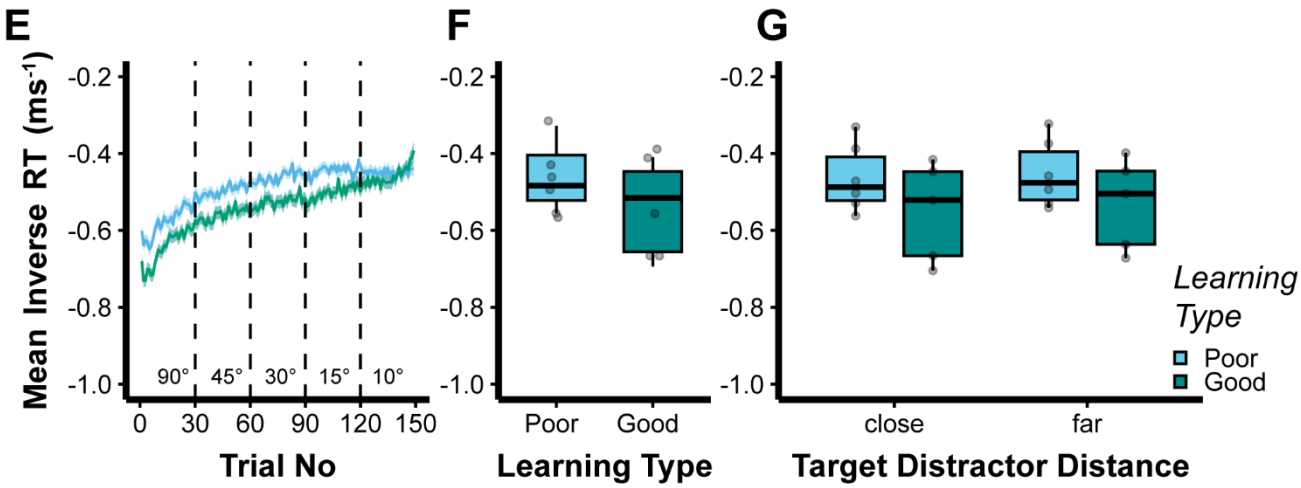

3.3 GABAergic pharmacology

To investigate the contribution of GABRA5 to VPL we administered the GABRA5 positive allosteric modulator (PAM) alogabat during task performance. To interrogate the specificity of the behavioral effects of this GABRA5-based compound we also administered two clinically available compounds: tiagabine, a GABA reuptake inhibitor and baclofen, a GABA B agonist.

As shown in Figure 4A, tiagabine had no significant effect on accuracy (compared to Veh: 0.5 mg/kg, Pr(>|z|) = 0.831, 2.5 mg/kg, Pr(>|z|) = 0.461, 7.5 mg/kg, Pr(>|z|) = 0.961). However, in good learners, tiagabine had a dose dependent effect on response latencies (main effect of dose: $F_{(3,161)} = 17.3$, Pr(>F) = $8.88e^{-10}$). Here, low (Veh-0.5 mg/kg: adj.p value = 0.0365) and middle doses (Veh-2.5 mg/kg: adj.p value = 0.0001) increased response speed whereas the highest dose slowed responding compared to all other doses (Veh-7.5 mg/kg: adj.p value = 0.031, 0.5 mg/kg-7.5 mg/kg: adj.p value < 0.0001, 2.5 mg/kg-7.5 mg/kg: adj.p value < 0.0001) (Figure 4B).

Administration of R-baclofen impacted accuracy in both learning groups (Figure 4C) (compared to Veh: 0.05 mg/kg, Pr(>|z|) = 0.862, 0.5 mg/kg, Pr(>|z|) = $2.89e^{-05}$, 1.5 mg/kg, Pr(>|z|) = 0.00182). Here, middle-dose R-baclofen improved “Good” learner accuracy (Good: Veh-0.5 mg/kg: adj.p value = 0.048), and had a positive effect on accuracy in “Poor” learners (Poor: Veh - 0.5 mg/kg: adj.p value = 0.0002, 0.05 mg/kg – 0.5 mg/kg: adj.p value = 0.0001). High-dose baclofen improved the accuracy of “Poor” leaners (Poor: Veh-1.5 mg/kg: adj.p value = 0.0099, Veh-0.5 mg/kg: adj.p value = 0.008) but this comparison was relatively low powered due to subject exclusion (Figure S6). Low dose R-baclofen had no impact on “Poor” learner accuracy (Poor: Veh-0.05 mg/kg: adj.p value = 0.998), but there was a positive trend associated with “Good” learner performance (Good: Veh-0.05 mg/kg: adj.p value = 0.0868). Whilst there was a main effect of R-baclofen dose on inverseRT ($F_{(3,139)} = 6.05$, Pr(>F) = $6.68e^{-04}$), this was limited to “Poor” learners only. Here, dose wise comparisons revealed faster responses at the intermediate dose (Poor: Veh-0.5 mg/kg: adj.p value = 0.0026), and slowing at high doses (Poor: Veh-1.5 mg/kg: adj.p value = 0.0014, 0.05-1.5 mg/kg: adj.p value < 0.0001, 0.5-1.5 mg/kg: adj.p value < 0.0001) compared to vehicle and low dose conditions (Figure 4D).

Like baclofen, alogabat administration modified accuracy in both learning groups (Veh-3 mg/kg, Pr(>|z|) = $1.30e^{-05}$, Veh-10 mg/kg, Pr(>|z|) = $9.87e^{-12}$, Veh-30 mg/kg, Pr(>|z|) =

0.479). Within groups, “Poor” learner accuracy demonstrated an ‘inverted-U’ dose-response with stepwise improvements in accuracy from vehicle at 3 mg/kg (Poor:Veh-3 mg/kg: adj.p value = 0.0001), and 10 mg/kg doses (Poor:Veh-10 mg/kg: adj.p value < 0.0001) whereas high dose exhibited no difference compared with the vehicle control group (Poor:Veh-30 mg/kg: adj.p value = 0.894). In contrast, a dose of 30 mg/kg alogabat improved “Good” learner accuracy (adj.p value = 0.0001) with lower doses showing comparable accuracy with the vehicle group (Figure 4E) (Veh-3 mg/kg: adj.p value = 0.701, Veh-10 mg/kg: adj.p value = 0.986). Like tiagabine, alogabat had significant effects on response latencies in “Good” learners only. Thus, a dose of 10 mg/kg resulted in faster responses compared with vehicle (Veh-10 mg/kg: adj.p value = 0.0275) and 3 mg/kg (3 -10 mg/kg: adj.p value = 0.0193), whilst 30 mg/kg slowed responding compared to the 10 mg/kg dose level (10-30 mg/kg: adj.p value < 0.0001) (Figure 4F).

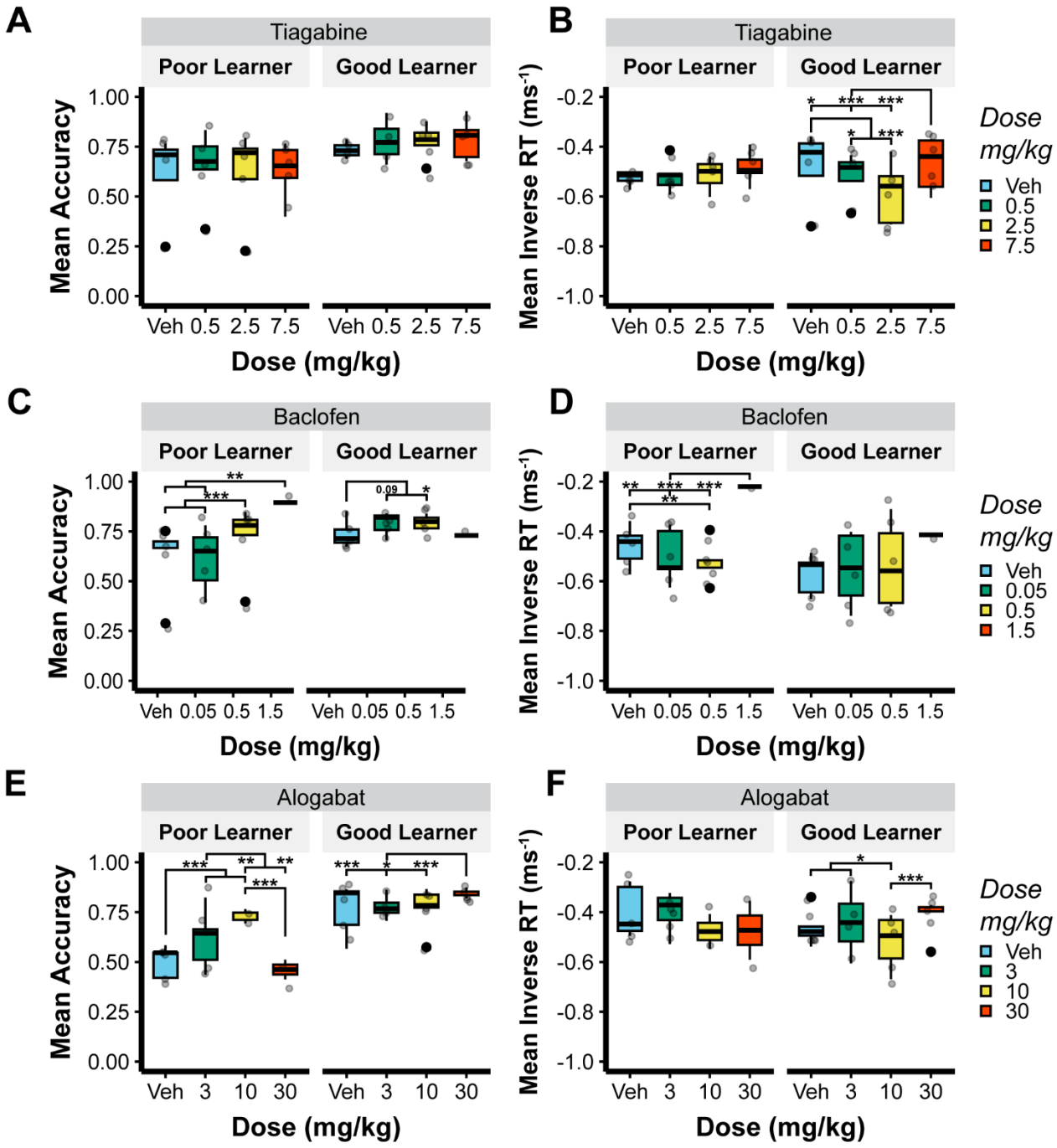

Figure 4 Baseline-dependent effects of GABAergic interventions on the VPL task
A Distribution of full task mean accuracy following the administration of the GAT-1 inhibitor tiagabine separated by learning group. **B** Distribution of full task mean inverseRT following the administration of the GAT-1 inhibitor tiagabine separated by learning group. **C** Distribution of full task mean accuracy following the administration of the GABA B agonist R-baclofen separated by learning group. **D** Distribution of full task mean inverseRT following the administration of GABA B agonist R-baclofen separated by learning group. **E** Distribution of full task mean accuracy following the administration of the GABRA5 positive allosteric modulator alogabat separated by learning group. **F** Distribution of full task mean inverseRT following the administration of the GABRA5 positive allosteric modulator alogabat separated by learning group.
Generalized linear mixed-effects model with binomial link **(A,C,E).** Linear mixed-effects model **(B,D,F)**. Boxplots denote median, interquartile range with whiskers extending to 1.5x IQR. Outliers denoted by solid points. Pairwise comparisons made via estimated marginal means to Vehicle condition in each case, within "Learning type". Effect sizes: "p value" = p<0.1, "*" = p<0.05, "**" = p<0.01, "***" = p<0.001**(B,D,F)** and as log-odds ratios **(A,C,E)**.

3.4 Relating perceptual performance to GABRA5 expression

To identify the putative substrates underlying the variability in alogabat's drug effects we next investigated GABRA5 expression in primary visual cortex (V1) and subregions of the mPFC (Cg1, PrL, IL – see Figure 5A) using Western immunoblot and RNA scope fluorescence in-situ-hybridisation (RNA Scope) (Figure 5B-D).

Western blot protein analysis highlighted an increased level of GABRA5 protein expression in the PrL of good learners (Poor - Good: p-value = 0.0393) (Figure 5E). We then assessed GABRA5 mRNA in selective subpopulations of inhibitory interneurons, specifically: parvalbumin (Pvalb)-, somatostatin (Sst)-, vasoactive intestinal peptide (VIP)- and excitatory pyramidal cells (slc17A7) in each target cortical region of interest. Statistical comparison between learning types revealed a greater number of GABRA5 and Sst co-expressing cells in the PrL of good learners (Poor - Good: adj.p value = 0.0006) (Figure 5F), an increased number of GABRA5 and Sst overlapping mRNA copies in the Cg1 and PrL of good learners (Cg1:Poor - Good: adj.p value = 0.0187, PrL: Poor - Good: adj.p value = 0.0038), and a greater number of GABRA5 and Pvalb overlapping mRNA copies in the PrL of good learners (Poor - Good: adj.p value = 0.0031) (Figure 5G). There was no difference in within-region total-DAPI derived learning-type cell counts (LT:Region - $F_{(3,22.4)}$ = 0.102, Pr(>F) = 0.958). All other comparisons were non-significant. A summary of the molecular quantification data is given in supplementary Table 2.

Figure 5: Relationship of GABRA5 expression with perceptual acuity and learning rate
A Schematic illustrations showing target regions of interest, left = primary visual cortex (V1) -5.6mm – -8.16 mm from bregma, right = prefrontal cortex (PFC) 4.6 mm – 2.52 mm from bregma. Sub-regions: anterior cingulate cortex (Cg1), prelimbic cortex (PrL), infralimbic cortex (IL). **B** Representative section of PFC showing fluorescent signal aligned with ROIs. **C** RNAscope assays from representative good versus poor learners on the VPL task. Scale bar 100 µm. Assay 1 GABRA5 (red); Pvalb (green); Sst (yellow): Assay 2 GABRA5 (red); slc17A7 (green); VIP (yellow). Arrows highlight cells expressing target probes in each case. **D** Representative Western-immunoblot gel for GABRA5 protein expression in good versus poor learning groups with actin as the housekeeper control for each ROI. **E** Statistical comparison of Western-immunoblot derived GABRA5 protein expression in cortical ROIs between stratified "learning types". **F** Cell-wise quantification of GABRA5 co-expression from RNAscope assays within inhibitory interneuron subtypes: parvalbumin (Pvalb), somatostatin (Sst), vasoactive intestinal peptide (VIP) and excitatory pyramidal cells (slc17A7) by "Learning type", per target cortical region. **G** Puncta-wise quantification of GABRA5 co-expression from RNAscope assays within inhibitory interneuron subtypes: parvalbumin (Pvalb), somatostatin (Sst), vasoactive intestinal peptide (VIP) and excitatory pyramidal cells (slc17A7) by "learning type" in target cortical regions. A modulus transformation (p=0.3) was applied to scale the RNAscope y-axes to enable better interpretability between high and low expression values on the same plot. mRNA coexpression values are displayed for each "learning type" as mean ± SEM per subject. RNAscope was performed using 2 assays to assess GABRA5 within (1: Pvalb, Sst, 2: VIP, slc17A7) highlighted with dashed line. Pairwise comparisons made via linear mixed-effects model to "poor learner" condition each case via estimated-marginal-means, within region and cell type: "p value" = p<0.1, "*" = p<0.05, "**" = p<0.01, "***" = p<0.001.

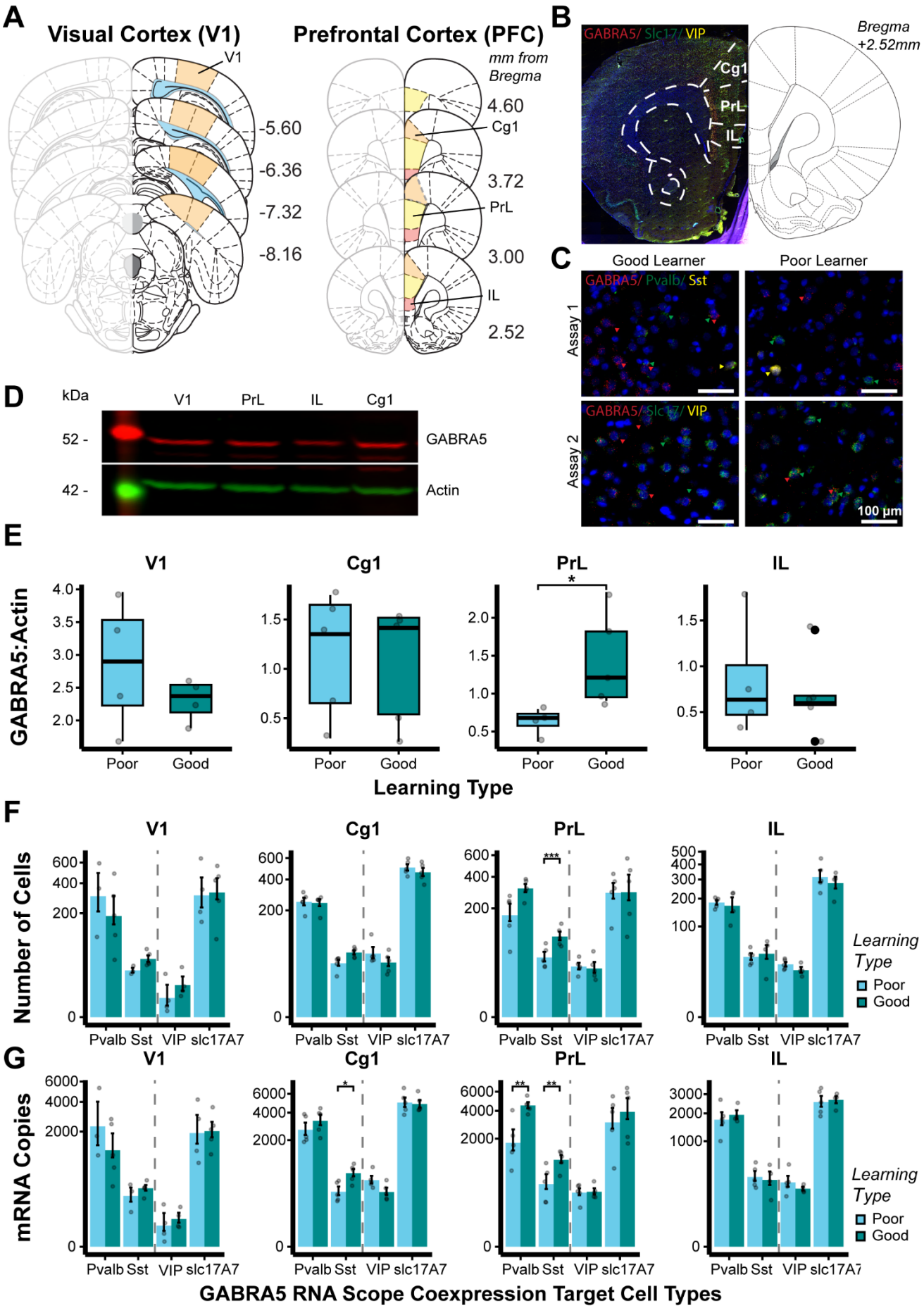

4.0 Discussion

In this study we investigated the role of inhibitory neurotransmission in VPL and specifically an underlying involvement of α5 subunit containing GABA-A receptors. Using a novel orientation discrimination task, we assessed the association between GABRA5 expression and task acquisition and validated our findings with selective GABAergic pharmacological agents in both male and female animals. We report that superior learning on a visual discrimination perceptual task is accompanied by increased GABRA5 expression in Sst and Pvalb interneuronal populations in the prelimbic subregion of the medial prefrontal cortex. Since VPL acuity in poor learners was improved following positive allosteric GABRA5 modulation during the early task sessions, our findings indicate that VPL may depend in part on optimal GABRA5 mediated inhibition in the prelimbic cortex early in the learning process.

4.1 Modelling perceptual learning and attentional load

Orientation discrimination is a commonly employed behavioral paradigm to investigate perceptual acuity in rodents[28,38] and humans[58,59]. However, cross-species translation is often challenged by differences in task configuration and decoding precisely how rodents solve tasks of this nature. To address these issues, we developed a novel progressive orientation discrimination paradigm to test rodent visual perceptual learning in a manner as close to human perceptual tasks as possible. Like virtual-reality or head-fixed running wheel approaches[60,61], we used progressive orientation discrimination as the perceptual challenge. However, unlike 2-choice perceptual tasks in rodents[62], we added a third stimulus. By simultaneously presenting target and distractor gratings close or far from one another, we not only reduced procedural location-based learning but also widened the window for pharmacological effects (from chance performance of 50% to 33%). In addition, the configuration of our novel task increased attentional demands[63], thus mimicking the high attentional load of equivalent VPL tasks in humans[64]. Crucially, our approach also preserved fine discrimination without restraint, facilitating naturalistic behavior and negating the limitations of head fixed approaches commonly used in go/no-go-based perceptual tasks. With these features, our task permitted the investigation and decoding of multiple components of visual perceptual learning whilst also enabling future temporally resolved neural recording techniques such as fiber photometry[65] and electrocorticography (ECoG)[66,67].

4.2 VPL variability is associated with GABRA5 expression in the prelimbic cortex

To investigate intrinsic differences in perceptual learning in our task, we stratified behavior at the conclusion of the pretraining stage. At this point in acquisition, stimulus reward associations (PT2+3), distractor interference tolerance (PT4, VD1-5), and spatial flexibility (PT2-VD5) could be assessed. Our approach aimed to separate the upper and lower tertiles of learning rate to determine whether GABRA5 expression in key components of the visual processing pathway were associated with task acquisition and could function as predictors of subsequent baseline performance.

VPL involves the integration of bottom-up sensory processing and coordinated responses from top-down attentional control mechanisms[68–73]. Our finding that higher GABRA5 protein expression in a subregion of the PFC – the PrL – is associated with faster perceptual learning indicates that top-down inhibitory control may be an important determinant of early contingency learning in this task. Supporting this notion, animals showing faster rates of learning were also more tolerant of a wider separation between the target and distractor stimuli, consistent with a role of the PrL in maintaining attentional focus in the face of distraction[74,75]. Indeed, higher cortical regions including the PFC and parietal association cortex (PC) are implicated in the control of interference suppression[76] in response to multiple simultaneously presented visual stimuli on such tasks as multiple-object-tracking (MOT)[77] and visual discrimination[78]. Such observations imply that top-down control processes may be necessary for acquiring attentional selection strategies to enable discriminative acuity in the present VPL task.

Within each session we found block-wise differences in VPL performance between fast and slower learning male and female rats, which diminished toward the most challenging discrimination block (10° from target). This finding suggests that whilst faster contingency learning during pretraining is beneficial in overall task performance, when the task reaches fine levels of discrimination, even robust interference suppression strategies are ineffective. Since the PrL contributes to the formation of stimulus reward action-associations and dynamic cue-outcome predictions when the stimulus is either ‘rewarded’ or ‘not rewarded’, rather than changes to its ‘value’[79,80] we suggest that when target and distractor stimuli converge in orientation, so too do their perceived values. Here, groupwise perceptual strategies recruited early in learning and putatively modulated by GABRA5 in the PrL may break down due to high levels of uncertainty between the perceived values of target and distractor stimuli. Instead, processing may depend more on bottom-up sensory integration

or other stimulus-value associated regions such as the orbitofrontal cortex[81,82]. However, it could also be argued that 10-degree discrimination represents a perceptual limit for rats in this task. Taken together, these findings suggest that PrL GABRA5 expression may enable faster acquisition of top-down stimulus-reward association weights and interference suppression strategies during pretraining. However, during late VPL, a limit is reached for fine discriminations that may be independent of GABRA5 in the PrL.

4.3 GABRA5 selective agents may alter performance by modifying tonic inhibitory activity

The pharmacological interventions in this study aimed to validate the observed differential expression of GABRA5 in the PrL of good and poor learners. To achieve this objective we administered a specific GABRA5 PAM, alogabat, and compared its effects to clinical compounds that potentiate metabolic (tiagabine) and post-synaptic tonic inhibitory activity (R-baclofen), both of which have demonstrated pro-cognitive effects in different contexts[83,84]. Here, we found a lack of efficacy in metabolic GABA potentiation with tiagabine, but a positive dose-dependent effect of baclofen on discriminative accuracy in both poor and good learning male rats. In contrast, alogabat elicited a dose-dependent enhancement in VPL performance that varied according to learning group and timing of administration.

Our findings with tiagabine and baclofen suggest that extracellular GABA levels do not impact task performance at nonsedative doses, but that moderate post-synaptic potentiation via the GABA B receptor improves perceptual acuity regardless of task acquisition rate whilst sparing side effects. However, the effects of alogabat are more challenging to interpret. It should be noted that administration timing of alogabat was variable, firstly between male and female animals (sessions 1-13 male, 16-23 female), and secondly, based on relative task experience between good and poor learning males (sessions: 1-8 poor, ~5-13 good) (Figure S10). We acknowledge this variation as a limitation but suggest the accompanied behavioural effects shed light on the time dependent mechanisms by which GABRA5 acts in this task.

Alogabat administration resulted in an apparent inverted-U dose response effect on accuracy in poor learning males, and a positive log-linear dose response in good learning males. Considering poor learning males were yet to asymptote during administration we suggest that potentiating GABRA5 in this window enables faster learning of the top-down

stimulus reward associations. Whereas, in good learning males which did not display asymptotic performance, refinements could only be made at the highest dose (details of session-wise baseline performance found in Figure S11). Whilst these responses relate to groupwise PrL GABRA5 expression, the similar performance effects of baclofen and alogabat in male rats suggests that alogabat may be modifying cortical tonic inhibition. Tonic GABA currents are typically viewed as constraining learning and memory while sharpening sensory processing (reviewed by Koh., et al. 2023)[85]. Although GABA B receptors contribute substantially to tonic inhibition, several extrasynaptic GABA A subtypes including GABRA5 also mediate shunting inhibition[45,86,87]. This GABA A-based mechanism has been proposed to narrow the temporal integration window of incoming signals, thereby increasing the signal-to-noise ratio and improving the fidelity of sensory representations[88,89]. In this context, pharmacological potentiation of GABRA5 would be expected to bias microcircuitry toward stability and noise-suppression, potentially enhancing distractor resistance. Indeed, consistent with the clinical indications of alogabat [52] and similar pro-cognitive GABRA5 PAMs [90,91] we suggest that modulating GABRA5 in this way may benefit refinements in early plastic learning periods that appear to rely on receptor expression presumably related to dynamic synaptic localisation.

Our pharmacological interventions support the notion that extrasynaptic GABRA5 receptors regulate a balance between stability and plasticity favouring stability for faster task acquisition. However, tuning by GABRA5 pharmacology during early exposure to the final task may enable long-term refinements of stimuli representations, which depend on intrinsic receptor expression. Moreover, once these representations are well trained, ceiling effects of increased tonic GABA inhibition is evident.

4.4 Sst and pvalb interneuron GABRA5 mRNA expression underlies behavioral and pharmacological variation

Our RNAScope findings indicate that higher GABRA5 expression in mPFC pvalb and Sst interneuron populations benefit early task learning and long-term baseline performance. Based on the established connections between GABRA5 and Sst interneurons with dendritic input gating refinement to pyramidal cells (PYR) [92–96], we posit that sensory signal-to-noise ratio and input integration mediated by these cells may be an important determinant of distractor suppression mediated by the PrL during VPL acquisition. A putative involvement of Pvalb interneurons also suggests GABRA5+ cells contribute to PrL recurrent inhibitory activity to fine tune the local E/I balance, thereby enhancing task

acquisition via trial-by-trial prediction error updates[97,98]. The absence of GABRA5 expression differences in VIP and slc17A7 expressing PYR cells potentially highlights canonical microcircuit mechanisms where VIP interneurons disinhibit PYR excitability through inhibition of Sst suppression of PYR cells and would be bypassed by increased tonic inhibition from GABRA5 expressing pvalb and Sst populations[16,92]. These findings suggest that GABRA5 clusters in Pvalb and Sst interneurons of the PrL functioning to bias the microcircuitry towards greater tonic inhibitory tuning of sensory input fidelity. This mechanism would account for faster learning in animals exhibiting a higher intrinsic expression of GABRA5.

The profound differences observed in the acquisition of the present VPL task in male and female rats precludes a meaningful comparison to be made in terms of drug effects and GABRA5 dependent mechanisms. The longer acquisition observed in female rats suggests females may be more susceptible to distraction interference than males. Indeed, a previous study also reported longer training periods of female rats in similar 3-stimuli operant task compared to males[99]. Additionally, we acknowledge that the timing of Alogabat administration renders stable performance vs learning effects inseparable. Although, we argue that based on the consistency of RNAScope findings across the cohort, the similarities in experienced animal responses to alogabat and baclofen, and the dynamic synaptic localisation of GABRA5 receptors, our results display useful learning-based findings on the contributions of GABRA5. Finally, our results present longitudinal behaviour, but static molecular readouts.

4.5 Conclusions

Overall, we report a convergent set of findings implicating GABRA5 mediated inhibitory processes during adaptive visually guided behaviors. We report a putative involvement of GABRA5 expressed Sst and pvalb interneurons of the PrL in a visual orientation discrimination task that involves set-shifting and simultaneous suppression of distractor stimuli in the visual field. We validated GABRA5's role in our task via comparing selective GABAergic agents between groups of animals stratified according to poor and good learning during early acquisition of the task. Our findings indicate that suppression of interference by the PrL may facilitate faster learning in animals exhibiting high expression of GABRA5 in PrL Sst and Pvalb expressing interneurons. Thus, in conclusion, GABRA5

expressed in the PrL may mediate tonic inhibitory control of excitatory sensory input to facilitate top-down learning of perceptual task contingencies.

Acknowledgements

This work was supported by the Wellcome Trust (223131/Z/21/Z) and a studentship from Boehringer Ingelheim Pharma. The experimental work was carried out under a Home Office Project Licence held by Prof. Dr. A. L. Milton.

Author Contributions

Conceptualization: MCDB. Experimental design: MCDB. Data analysis: MCDB, OSRPS, LVW. Investigation: MCDB, EP, CVS, LMP. Visualization: MCDB, EP, CVS, LMP. Supervision: JFdH, JWD. Writing–original draft: MCDB JWD. Writing–review & editing: all authors

Conflicts of Interest

The authors declare no competing interests

5.0 References

1. Ahissar, M. & Hochstein, S. Task difficulty and the specificity of perceptual learning. *Nature* **387**, 401–6 (1997).
2. Ball, K. & Sekuler, R. Direction-specific improvement in motion discrimination. *Vision Res.* **27**, 953–965 (1987).
3. Karni, A. & Sagi, D. Where practice makes perfect in texture discrimination: evidence for primary visual cortex plasticity. *Proceedings of the National Academy of Sciences* **88**, 4966–4970 (1991).
4. Shiu, L. P. & Pashler, H. Improvement in line orientation discrimination is retinally local but dependent on cognitive set. *Percept. Psychophys.* **52**, 582–8 (1992).
5. Hubel, D. H. & Wiesel, T. N. Receptive fields, binocular interaction and functional architecture in the cat's visual cortex. *J. Physiol.* **160**, 106–154 (1962).
6. Schoups, A., Vogels, R., Qian, N. & Orban, G. Practising orientation identification improves orientation coding in V1 neurons. *Nature* **412**, 549–553 (2001).
7. Hubel, D. H. & Wiesel, T. N. Receptive fields and functional architecture of monkey striate cortex. *J. Physiol.* **195**, 215–243 (1968).
8. Mukai, I. *et al.* Activations in Visual and Attention-Related Areas Predict and Correlate with the Degree of Perceptual Learning. *The Journal of Neuroscience* **27**, 11401–11411 (2007).
9. Kahnt, T., Grueschow, M., Speck, O. & Haynes, J.-D. Perceptual Learning and Decision-Making in Human Medial Frontal Cortex. *Neuron* **70**, 549–559 (2011).
10. Jing, R., Yang, C., Huang, X. & Li, W. Perceptual learning as a result of concerted changes in prefrontal and visual cortex. *Current Biology* **31**, 4521-4533.e3 (2021).
11. Ganguly, K., Schinder, A. F., Wong, S. T. & Poo, M. ming. GABA itself promotes the developmental switch of neuronal GABAergic responses from excitation to inhibition. *Cell* **105**, 521–532 (2001).
12. Kirmse, K. *et al.* GABA depolarizes immature neurons and inhibits network activity in the neonatal neocortex in vivo. *Nat. Commun.* **6**, (2015).
13. Froemke, R. C. Plasticity of cortical excitatory-inhibitory balance. *Annu. Rev. Neurosci.* **38**, 195–219 (2015).
14. van Versendaal, D. & Levelt, C. N. Inhibitory interneurons in visual cortical plasticity. *Cellular and Molecular Life Sciences* **73**, 3677–3691 (2016).
15. Desrosiers, J. & Basha, D. Cortical Inhibition, Plasticity, and Sleep. *The Journal of Neuroscience* **43**, 523–525 (2023).
16. Tremblay, R., Lee, S. & Rudy, B. GABAergic Interneurons in the Neocortex: From Cellular Properties to Circuits. *Neuron* **91**, 260–292 (2016).
17. Hollestein, V. *et al.* Excitatory/inhibitory imbalance in autism: the role of glutamate and GABA gene-sets in symptoms and cortical brain structure. *Transl. Psychiatry* **13**, 1–9 (2023).
18. Cooper, R. A. *et al.* Reduced hippocampal functional connectivity during episodic memory retrieval in autism. *Cerebral Cortex* **27**, 888–902 (2017).
19. Lesh, T. A., Niendam, T. A., Minzenberg, M. J. & Carter, C. S. Cognitive control deficits in schizophrenia: Mechanisms and meaning. *Neuropsychopharmacology* **36**, 316–338 (2011).
20. RA McCutcheon, R. K. P. M. Cognitive impairment in schizophrenia: aetiology, pathophysiology, and treatment. *Mol. Psychiatry* **28**, 1902–1918 (2023).
21. Howes, O. D., Bukala, B. R. & Beck, K. Schizophrenia: from neurochemistry to circuits, symptoms and treatments. *Nature Reviews Neurology 2023 20:1* **20**, 22–35 (2023).
22. van Hugte, E. J. H., Schubert, D. & Kasri, N. N. E/I balance in epilepsies and neurodevelopmental disorders: depolarizing GABA as a common mechanism. *Epilepsia* 1–15 (2023) doi:10.1111/epi.17651.
23. Ferguson, B. R. & Gao, W. J. Pv interneurons: critical regulators of E/I balance for prefrontal cortex-dependent behavior and psychiatric disorders. *Front. Neural Circuits* **12**, (2018).
24. Mueller-Buehl, C., Wegrzyn, D., Bauch, J. & Faissner, A. Regulation of the E/I-balance by the neural matrisome. *Front. Mol. Neurosci.* **16**, (2023).

25. Kaar, S. J., Nottage, J. F., Angelescu, I., Marques, T. R. & Howes, O. D. Gamma Oscillations and Potassium Channel Modulation in Schizophrenia: Targeting GABAergic Dysfunction. *Clin. EEG Neurosci.* **55**, 203–213 (2024).
26. Hoftman, G. D. *et al.* Altered cortical expression of GABA-related genes in schizophrenia: Illness progression vs developmental disturbance. *Schizophr. Bull.* **41**, 180–191 (2015).
27. Marín, O. Parvalbumin interneuron deficits in schizophrenia. *Eur Neuropsychopharmacol* **82**, 44–52 (2024).
28. Poort, J. *et al.* Learning and attention increase visual response selectivity through distinct mechanisms. *Neuron* **110**, 686–697 (2022).
29. Yazaki-Sugiyama, Y., Kang, S., Câteau, H., Fukai, T. & Hensch, T. K. Bidirectional plasticity in fast-spiking GABA circuits by visual experience. *Nature* **462**, 218–21 (2009).
30. Kuchibhotla, K. V *et al.* Parallel processing by cortical inhibition enables context-dependent behavior. *Nat. Neurosci.* **20**, 62–71 (2017).
31. Kato, H. K., Gillet, S. N. & Isaacson, J. S. Flexible Sensory Representations in Auditory Cortex Driven by Behavioral Relevance. *Neuron* **88**, 1027–1039 (2015).
32. Cheng, R. *et al.* A disinhibitory microcircuit in the temporal association cortex for fear retrieval to pure tones. *Sci. Rep.* **15**, 1–16 (2025).
33. Khan, A. G. *et al.* Distinct learning-induced changes in stimulus selectivity and interactions of GABAergic interneuron classes in visual cortex. *Nat. Neurosci.* **21**, 851–859 (2018).
34. Myers-Joseph, D., Wilmes, K. A., Fernandez-Otero, M., Clopath, C. & Khan, A. G. Disinhibition by VIP interneurons is orthogonal to cross-modal attentional modulation in primary visual cortex. *Neuron* **112**, 628-645.e7 (2024).
35. Aime, M. *et al.* Paradoxical somatodendritic decoupling supports cortical plasticity during REM sleep. *Science (1979).* **376**, 724–730 (2022).
36. Snyder, A. C., Morais, M. J. & Smith, M. A. Dynamics of excitatory and inhibitory networks are differentially altered by selective attention. *J. Neurophysiol.* **116**, 1807–1820 (2016).
37. Snyder, A. C., Yu, B. M. & Smith, M. A. A Stable Population Code for Attention in Prefrontal Cortex Leads a Dynamic Attention Code in Visual Cortex. *Journal of Neuroscience* **41**, 9163–9176 (2021).
38. Speed, A., Del Rosario, J., Mikail, N. & Haider, B. Spatial attention enhances network, cellular and subthreshold responses in mouse visual cortex. *Nat. Commun.* **11**, 505 (2020).
39. Raven, F. & Aton, S. J. The Engram's Dark Horse: How Interneurons Regulate State-Dependent Memory Processing and Plasticity. *Front. Neural Circuits* **15**, (2021).
40. Olsen, R. W. & Sieghart, W. GABAA receptors: Subtypes provide diversity of function and pharmacology. *Neuropharmacology* **56**, 141–148 (2009).
41. Weir, C. J. Ion channels, receptors, agonists and antagonists. *Anaesthesia & Intensive Care Medicine* **17**, 645–651 (2016).
42. Pinard, A., Seddik, R. & Bettler, B. GABA B receptors. Physiological functions and mechanisms of diversity. in *Advances in Pharmacology* vol. 58 231–255 (2010).
43. Kohl, M. M. & Paulsen, O. The roles of GABA B receptors in cortical network activity. in *Advances in Pharmacology* vol. 58 205–229 (Academic Press Inc., 2010).
44. Prut, L. *et al.* A reduction in hippocampal GABA $_A$ receptor α5 subunits disrupts the memory for location of objects in mice. *Genes Brain Behav.* **9**, 478–488 (2010).
45. Caraiscos, V. B. *et al.* Tonic inhibition in mouse hippocampal CA1 pyramidal neurons is mediated by α5 subunit-containing γ-aminobutyric acid type A receptors. *Proceedings of the National Academy of Sciences* **101**, 3662–3667 (2004).
46. Zarnowska, E. D., Keist, R., Rudolph, U. & Pearce, R. A. GABAA receptor α5 subunits contribute to GABA A,slow synaptic inhibition in mouse hippocampus. *J. Neurophysiol.* **101**, 1179–1191 (2009).
47. Engin, E. *et al.* Tonic Inhibitory Control of Dentate Gyrus Granule Cells by α5-Containing GABA $_A$ Receptors Reduces Memory Interference. *The Journal of Neuroscience* **35**, 13698–13712 (2015).
48. Serwanski, D. R. *et al.* Synaptic and nonsynaptic localization of GABAA receptors containing the alpha5 subunit in the rat brain. *J. Comp. Neurol.* **499**, 458–70 (2006).

49. Panzanelli, P. *et al.* Distinct mechanisms regulate GABA A receptor and gephyrin clustering at perisomatic and axo-axonic synapses on CA1 pyramidal cells. *J. Physiol.* **589**, 4959–4980 (2011).
50. Davenport, C. M. *et al.* Relocation of an Extrasynaptic GABAA Receptor to Inhibitory Synapses Freezes Excitatory Synaptic Strength and Preserves Memory. *Neuron* **109**, 123-134.e4 (2021).
51. Crijns, E. & Op de Beeck, H. The Visual Acuity of Rats in Touchscreen Setups. *Vision* **4**, 4 (2019).
52. Cecere, G. *et al.* Preclinical pharmacology of alogabat: a novel GABAA-α5 positive allosteric modulator targeting neurodevelopmental disorders with impaired GABAA signaling. *Front. Pharmacol.* **16**, 1626078 (2025).
53. Horner, A. E. *et al.* The touchscreen operant platform for testing learning and memory in rats and mice. *Nat. Protoc.* **8**, 1961–1984 (2013).
54. Wang, F. *et al.* RNAscope. *The Journal of Molecular Diagnostics* **14**, 22–29 (2012).
55. Velazquez-Sanchez, C., Muresan, L., Marti-Prats, L. & Belin, D. The development of compulsive coping behaviour is associated with a downregulation of Arc in a Locus Coeruleus neuronal ensemble. *Neuropsychopharmacology* **48**, 653–663 (2023).
56. Schindelin, J. *et al.* Fiji: An open-source platform for biological-image analysis. *Nature Methods* vol. 9 676–682 Preprint at https://doi.org/10.1038/nmeth.2019 (2012).
57. R: The R Project for Statistical Computing. https://www.r-project.org/.
58. Jia, K. *et al.* Visual perceptual learning modulates decision network in the human brain: The evidence from psychophysics, modeling, and functional magnetic resonance imaging. *J. Vis.* **18**, 9 (2018).
59. Edden, R. A. E., Muthukumaraswamy, S. D., Freeman, T. C. A. & Singh, K. D. Orientation Discrimination Performance Is Predicted by GABA Concentration and Gamma Oscillation Frequency in Human Primary Visual Cortex. *The Journal of Neuroscience* **29**, 15721–15726 (2009).
60. Poort, J. *et al.* Learning Enhances Sensory and Multiple Non-sensory Representations in Primary Visual Cortex. *Neuron* **86**, 1478–1490 (2015).
61. Wal, A., Klein, F. J., Born, G., Busse, L. & Katzner, S. Evaluating Visual Cues Modulates Their Representation in Mouse Visual and Cingulate Cortex. *The Journal of Neuroscience* **41**, 3531–3544 (2021).
62. Sale, A. *et al.* Visual perceptual learning induces long-term potentiation in the visual cortex. *Neuroscience* **172**, 219–225 (2011).
63. Yoo, S. A., Martinez-Trujillo, J. C., Treue, S., Tsotsos, J. K. & Fallah, M. Attention to visual motion suppresses neuronal and behavioral sensitivity in nearby feature space. *BMC Biol.* **20**, 1–19 (2022).
64. Edden, R. A. E., Muthukumaraswamy, S. D., Freeman, T. C. A. & Singh, K. D. Orientation discrimination performance is predicted by GABA concentration and gamma oscillation frequency in human primary visual cortex. *Journal of Neuroscience* **29**, 15721–15726 (2009).
65. Simpson, E. H. *et al.* Lights, fiber, action! A primer on in vivo fiber photometry. *Neuron* **0**, (2023).
66. Xie, K. *et al.* Portable wireless electrocorticography system with a flexible microelectrodes array for epilepsy treatment. *Sci. Rep.* **7**, 1–8 (2017).
67. Proctor, C. M. *et al.* An Electrocorticography Device with an Integrated Microfluidic Ion Pump for Simultaneous Neural Recording and Electrophoretic Drug Delivery In Vivo. *Adv. Biosyst.* **3**, e1800270–e1800270 (2018).
68. Barbera, D., Priebe, N. J. & Glickfeld, L. L. Feedforward mechanisms of cross-orientation interactions in mouse V1. *Neuron* **110**, 297-311.e4 (2022).
69. Bastos, A. M. *et al.* Visual areas exert feedforward and feedback influences through distinct frequency channels. *Neuron* **85**, 390–401 (2015).
70. Kok, P., Bains, L. J., Van Mourik, T., Norris, D. G. & De Lange, F. P. Selective Activation of the Deep Layers of the Human Primary Visual Cortex by Top-Down Feedback. *Current Biology* **26**, 371–376 (2016).
71. Huh, C. Y. L., Peach, J. P., Bennett, C., Vega, R. M. & Hestrin, S. Feature-Specific Organization of Feedback Pathways in Mouse Visual Cortex. *Current Biology* **28**, 114-120.e5 (2018).
72. Schäfer, R., Vasilaki, E. & Senn, W. Perceptual Learning via Modification of Cortical Top-Down Signals. *PLoS Comput. Biol.* **3**, e165 (2007).

73. Zhang, S. *et al.* Selective attention. Long-range and local circuits for top-down modulation of visual cortex processing. *Science (1979).* **345**, 660–665 (2014).
74. Sharpe, M. J. & Killcross, S. The Prelimbic Cortex Contributes to the Down-Regulation of Attention Toward Redundant Cues. *Cerebral Cortex* **24**, 1066–1074 (2014).
75. Auger, M. L., Meccia, J. & Floresco, S. B. Regulation of sustained attention, false alarm responding and implementation of conditional rules by prefrontal GABAA transmission: comparison with NMDA transmission. *Psychopharmacology (Berl).* **234**, 2777–2792 (2017).
76. Wöstmann, M. *et al.* Ten simple rules to study distractor suppression. *Prog. Neurobiol.* **213**, 102269 (2022).
77. Meyerhoff, H. S., Papenmeier, F. & Huff, M. Studying visual attention using the multiple object tracking paradigm: A tutorial review. *Atten. Percept. Psychophys.* **79**, 1255–1274 (2017).
78. Frangou, P. *et al.* Learning to optimize perceptual decisions through suppressive interactions in the human brain. *Nat. Commun.* **10**, 1–12 (2019).
79. Ostlund, S. B. & Balleine, B. W. Lesions of Medial Prefrontal Cortex Disrupt the Acquisition But Not the Expression of Goal-Directed Learning. *The Journal of Neuroscience* **25**, 7763–7770 (2005).
80. Niedringhaus, M. & West, E. A. Prelimbic cortex neural encoding dynamically tracks expected outcome value. *Physiol. Behav.* **256**, 113938 (2022).
81. Gourley, S. L., Zimmermann, K. S., Allen, A. G. & Taylor, J. R. The Medial Orbitofrontal Cortex Regulates Sensitivity to Outcome Value. *The Journal of Neuroscience* **36**, 4600–4613 (2016).
82. Marquardt, K., Sigdel, R. & Brigman, J. L. Touch-screen visual reversal learning is mediated by value encoding and signal propagation in the orbitofrontal cortex. *Neurobiol. Learn. Mem.* **139**, 179–188 (2017).
83. Sałat, K. *et al.* The effect of GABA transporter 1 (GAT1) inhibitor, tiagabine, on scopolamine-induced memory impairments in mice. *Pharmacological Reports* **67**, 1155–1162 (2015).
84. Stoppel, L. J. *et al.* R-Baclofen Reverses Cognitive Deficits and Improves Social Interactions in Two Lines of 16p11.2 Deletion Mice. *Neuropsychopharmacology* **43**, 513–524 (2018).
85. Koh, W., Kwak, H., Cheong, E. & Lee, C. J. GABA tone regulation and its cognitive functions in the brain. *Nat Rev Neurosci* **24**, 523–39 (2023).
86. Farrant, M. & Nusser, Z. Variations on an inhibitory theme: phasic and tonic activation of GABA(A) receptors. *Nat. Rev. Neurosci.* **6**, 215–29 (2005).
87. Perez-Sanchez, J. *et al.* α5GABAA Receptors Mediate Tonic Inhibition in the Spinal Cord Dorsal Horn and Contribute to the Resolution Of Hyperalgesia. *J. Neurosci. Res.* **95**, 1307–1318 (2017).
88. Pavlov, I., Savtchenko, L. P., Kullmann, D. M., Semyanov, A. & Walker, M. C. Outwardly rectifying tonically active GABAA receptors in pyramidal cells modulate neuronal offset, not gain. *J. Neurosci.* **29**, 15341–15350 (2009).
89. Brickley, S. G. & Mody, I. Extrasynaptic GABA A Receptors: Their Function in the CNS and Implications for Disease. *Neuron* **73**, 23–34 (2012).
90. Bernardo, A. M. *et al.* Procognitive and neurotrophic benefits of α5-GABA-A receptor positive allosteric modulation in a β-amyloid deposition mouse model of Alzheimer's disease pathology. *Neurobiol. Aging* **147**, 49–59 (2025).
91. Koh, M. T., Rosenzweig-Lipson, S. & Gallagher, M. Selective GABAA α5 positive allosteric modulators improve cognitive function in aged rats with memory impairment. *Neuropharmacology* **64**, 145–152 (2013).
92. Pfeffer, C. K., Xue, M., He, M., Huang, Z. J. & Scanziani, M. Inhibition of inhibition in visual cortex: the logic of connections between molecularly distinct interneurons. *Nature Neurosci.* **16**, 1068–1076 (2013).
93. Cao, J.-W., Guan, W., Yu, Y.-C. & Fu, Y. Synaptic Transmission from Somatostatin-expressing Interneurons to Excitatory Neurons Mediated by α5-subunit-containing GABAA Receptors in the Developing Visual Cortex. *Neuroscience* **449**, 147–156 (2020).
94. Huang, Y. Feature selective inhibitory mechanisms enable expectation suppression in cortical microcircuits. *Scientific Reports 2025 15:1* **15**, 44597- (2025).

95. Fee, C. *et al.* Behavioral Deficits Induced by Somatostatin-Positive GABA Neuron Silencing Are Rescued by Alpha 5 GABA-A Receptor Potentiation. *International Journal of Neuropsychopharmacology* **24**, 505–518 (2021).
96. Schulz, J. M., Knoflach, F., Hernandez, M.-C. & Bischofberger, J. Dendrite-targeting interneurons control synaptic NMDA-receptor activation via nonlinear α5-GABAA receptors. *Nat. Commun.* **9**, 3576 (2018).
97. Znamenskiy, P. *et al.* Functional specificity of recurrent inhibition in visual cortex. *Neuron* **112**, 991-1000.e8 (2024).
98. Jia, K. *et al.* Recurrent inhibition refines mental templates to optimize perceptual decisions. *Sci. Adv.* **10**, 31 (2024).
99. Kutash, L. A. *et al.* Sustained attention performance deficits in the three-choice serial reaction time task in male and female rats after experimental brain trauma. *Brain Res.* **1808**, 148336 (2023).